# Reducing host aldose reductase activity promotes neuronal differentiation of transplanted neural stem cells at spinal cord injury sites and facilitates locomotion recovery

### From the Contents

Kun Zhang[1, 2, #], Wen-Can Lu[3, #], Ming Zhang[1], Qian Zhang[4], Pan-Pan Xian[1], Fang-Fang Liu[1], Zhi-Yang Chen[5], Chung Sookja Kim[6], Sheng-Xi Wu[1], Hui-Ren Tao[3, *], Ya-Zhou Wang[1, *]

**Graphical Abstract** *Aldose reductase (AR) inhibitors with neural stem cell (NSC) transplantation for the treatment of spinal cord injury*
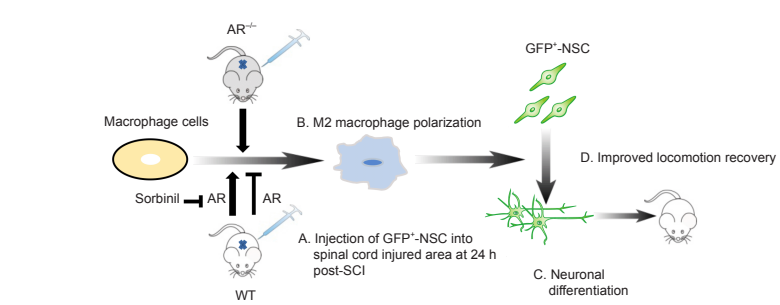
## Abstract

Neural stem cell (NSC) transplantation is a promising strategy for replacing lost neurons following spinal cord injury. However, the survival and differentiation of transplanted NSCs is limited, possibly owing to the neurotoxic inflammatory microenvironment. Because of the important role of glucose metabolism in M1/M2 polarization of microglia/macrophages, we hypothesized that altering the phenotype of microglia/macrophages by regulating the activity of aldose reductase (AR), a key enzyme in the polyol pathway of glucose metabolism, would provide a more beneficial microenvironment for NSC survival and differentiation. Here, we reveal that inhibition of host AR promoted the polarization of microglia/macrophages toward the M2 phenotype in lesioned spinal cord injuries. M2 macrophages promoted the differentiation of NSCs into neurons *in vitro*. Transplantation of NSCs into injured spinal cords either deficient in AR or treated with the AR inhibitor sorbinil promoted the survival and neuronal differentiation of NSCs at the injured spinal cord site and contributed to locomotor functional recovery. Our findings suggest that inhibition of host AR activity is beneficial in enhancing the survival and neuronal differentiation of transplanted NSCs and shows potential as a treatment of spinal cord injury.

**Key Words:** aldose reductase; functional recovery; inflammation; macrophage; microglia; neural stem cell transplantation; neuronal differentiation; polarization; spinal cord injury

## Introduction

Spinal cord injury (SCI) is the leading cause of paralysis in young people. There are approximately 250,000 to 500,000 new cases of SCI per year, globally (World Health Organization, 2013). Damage caused by the primary injury leads to secondary injury, which includes progressive neuronal loss, axonal degeneration and demyelination, and chronic inflammation and reactive gliosis. These processes usually lead to enlargement of the lesion area, which may cause a spinal cavity to form (Venkatesh et al., 2019). Among these pathological changes, neuronal loss has long been thought as irreversible, as there is no endogenous neurogenesis in the spinal

[1]Department of Neurobiology and Institute of Neurosciences, School of Basic Medicine, Fourth Military Medical University, Xi'an, Shaanxi Province, China; [2]Key Laboratory of Spine and Spinal Cord Injury Repair and Regeneration, Tongji University, Shanghai, China; [3]Department of Spine Surgery, Shenzhen University General Hospital, Shenzhen, Guangdong Province, China; [4]Department of Neurology, Hainan Hospital of Chinese PLA General Hospital, Sanya, Hainan Province, China; [5]Department of Anesthesiology, Tangdu Hospital, Fourth Military Medical University, Xi'an, Shaanxi Province, China; [6]Faculty of Medicine, Macau University of Science and Technology, Macau Special Administrative Region, China
*Correspondence to: Ya-Zhou Wang, MD, yazhouw@fmmu.edu.cn; Hui-Ren Tao, MD, huiren_tao@163.com.
https://orcid.org/0000-0002-7116-2395 (Ya-Zhou Wang)
#Both authors contribute equally to the work.

*How to cite this article:* Zhang K, Lu WC, Zhang M, Zhang Q, Xian PP, Liu FF, Chen ZY, Kim CS, Wu SX, Tao HR, Wang YZ (2022) Reducing host aldose reductase activity promotes neuronal differentiation of transplanted neural stem cells at spinal cord injury sites and facilitates locomotion recovery. Neural Regen Res 17(8):1814-1820.

cord after injury (Sabelström et al., 2013). Therefore, replenishing lost neurons and filling the spinal cavity are essential to the restoration of neural connections and promotion of functional recovery.

In the past decade, Schwann cells, neural stem cells (NSCs), mesenchymal stem cells, oligodendrocyte precursor cells, or olfactory ensheathing cells have been the focus for transplantation treatments for SCI, with the aim of alleviating secondary injury and promoting regeneration (Assinck et al., 2017; Liu et al., 2021; Wang et al., 2021). Among these cell types, NSC transplantation is advantageous, as NSCs can differentiate into neurons, astrocytes and oligodendrocytes, and these progenies assimilate easily into spinal tissue (Lu et al., 2014). Recently, it has been shown that NSCs grafted to a lesion area have poor survival and differentiation (Fan et al., 2018), particularly in the chronic inflammatory microenvironment of injured spinal cord (Orr and Gensel, 2018).

Aldose reductase (AR) is a core enzyme in the polyol pathway of glucose metabolism (Alexiou et al., 2009). Upregulation of AR is commonly observed in diabetic hyperglycemia and is strongly associated with activation of microglia/macrophages in cases of diabetic retinopathy (Albers and Pop-Busui, 2014; Chang et al., 2019). Inhibition of AR activity inhibits inflammation in multiple diseases (Quattrini and La Motta, 2019). In the spinal cord, AR is mainly upregulated in microglia/macrophages after injury (Zhang et al., 2016). Considering that glucose metabolism plays an essential role in the M1–M2 switch of microglia/macrophages (Stunault et al., 2018), we speculated that modulation of AR activity may change the phenotype of microglia/macrophages, thus offering a beneficial microenvironment for NSC transplantation. We tested this hypothesis by transplanting NSCs in AR-deficient or AR-inhibited mice.

## Materials and Methods

### Animals
We have previously generated AR-deficient mice (Ho et al., 2000). Green fluorescent protein (GFP) transgenic mice were purchased from the Shanghai Laboratory Animal Center, Shanghai, China, and bred in our animal facility. C57BL/6J mice were obtained from the Animal Center of the Fourth Military Medical University (Air Force Medical University), Xi'an, China (license No. SCXK (Shan) 2019-001). The protocols for all animal experiments were approved by the Animal Care and Use Committee of the Fourth Military Medical University (approval No. IACUC-20180907) on September 7, 2018, and the experiments were performed according to the guidelines of the Animal Care and Use Committee of the Fourth Military Medical University. A total of 288 mice were used in the present study, including 28 female C57BL/6J mice (days 12–14 of pregnancy) for primary culture, 20 female GFP transgenic mice (days 12–14 of pregnancy) for primary culture, 180 male C57BL/6J mice (6–8 weeks old) for SCI, and 60 male AR-deficient mice (6–8 weeks old) for SCI. All experiments were designed and reported according to the Animal Research: Reporting of *In Vivo* Experiments (ARRIVE) guidelines (Abecassis et al., 2020; Carter et al., 2020).

### Primary cell culture and treatment
#### Neural stem cell (NSC) culture
GFP transgenic mice at days 12–14 of pregnancy were sacrificed by euthanasia with 1% sodium pentobarbital intraperitoneally (60–80 mg/kg, Cat# P3761; MilliporeSigma, Burlington, MA, USA). A cesarean section was performed, and the embryos were carefully removed. Spinal cords were dissected under sterile conditions. The meninges were peeled off, and the spinal tissue was cut into small blocks of 1 mm³. Tissues were digested with 0.125% trypsin (Thermo Fisher Scientific, Waltham, MA, USA) containing 0.02% ethylenediaminetetraacetic acid (Thermo Fisher Scientific). The isolated primary cells were cultured in Neurobasal medium (Thermo Fisher Scientific) supplemented with 20–40 ng/mL epithelial growth factor (PeproTech, Cranbury, NJ, USA), 10–20 ng/mL fibroblast growth factor (PeproTech), 2% B-27 (Thermo Fisher Scientific), and 1% N2 supplement (Thermo Fisher Scientific). The medium was refreshed every other day. After 5–7 days *in vitro*, neurospheres were digested and passaged. We used neurospheres of the second or third passage for all subsequent experiments.

#### Culture of bone marrow macrophages
Adult C57BL/6J mice were sacrificed by euthanasia with 1% sodium pentobarbital intraperitoneally (60–80 mg/kg). Bone marrow cells were isolated from the femurs and tibias of the mice. After lysis with red blood cell lysis buffer (Cat# CW0613S; CWBIO, Beijing, China), cells were seeded in Dulbecco's modified Eagle's medium (Thermo Fisher Scientific) containing 0.1% β-mercaptoethanol (MilliporeSigma), 1% 4-(2-hydroxyethyl)piperazine-1-ethanesulfonic acid (MilliporeSigma), 20 ng/mL macrophage colony-stimulating factor (Cat# 315-02; PeproTech), and 10% fetal bovine serum (FBS; Thermo Fisher Scientific). After 10 days *in vitro*, nonadherent cells were removed by suction. Adherent cells were immunostained for ionized calcium-binding adapter molecule 1 to assess the purity of the macrophages (data not shown). Adherent cells were treated with lipopolysaccharides (100 ng/mL; PeproTech) and interferon-γ (20 ng/mL; PeproTech) to induce the M1 phenotype or treated with interleukin-4 (20 ng/mL; PeproTech) to induce the M2 phenotype (Zhang et al., 2016). One day later, the lipopolysaccharides, interferon-γ, and interleukin 4 were removed and Neurobasal medium was added. Conditioned medium (CM) was collected 24 hours later. Untreated macrophages were regarded as the M0 phenotype.

### NSC differentiation
Neurospheres were digested to isolate NSCs, and the NSCs were seeded onto dishes precoated with poly-L-lysine (25 μg/mL, Cat# P6282; MilliporeSigma) for 4 hours at 37°C. The cells were divided into three groups and cultured with M0-CM containing 2% FBS, M1-CM containing 2% FBS, or M2-CM containing 2% FBS, respectively, for 5 days.

### Spinal cord contusion and treatment
Adult male C57BL/6J mice were anesthetized with 1% sodium pentobarbital intraperitoneally (60–80 mg/kg) before surgery. After bilateral laminectomy of T8–T9, the T8 vertebra was crushed for 20 seconds using forceps with a tip gap of 0.2 mm, as previously described (Fan et al., 2013). Bladder massage to aid urination was conducted once or twice per day after surgery. Dorsal laminectomy without spinal cord crushing was carried out for the sham control group. SCI mice were divided into four groups: wild type (WT) + NSC transplantation (*n* = 60), WT + NSC transplantation + sorbinil (*n* = 60), AR + NSC transplantation (*n* = 30), and AR + NSC transplantation + phosphate-buffered saline (PBS) (*n* = 30 mice). For transplantation, NSCs were digested into a single cell suspension. NSCs ($1 \times 10^6$ cells, 2 μL) were injected into two regions of the crushed site (0.2 mm to the right and left of the dorsal midline at 0.3 mm depth) 24 hours after SCI using a stereotaxic apparatus (Cat# 68507; RWD Life Science Co., Shenzhen, China).

Three injections of 100 μM sorbinil (a widely used inhibitor of AR (Chang et al., 2019), Cat# S7701; MilliporeSigma) were made. The first (2 μL) was injected *in situ* immediately after SCI. The second (10 μL) was injected intraperitoneally immediately after NSC transplantation. The third (10 μL) was injected intraperitoneally 2 days post-injury. The same volume of PBS was used as the vehicle control.

### Immunohistochemistry
Arginase-1 (Arg-1) is a marker of M2 microglia/macrophages, inducible nitric oxide synthase (iNOS) is a marker of M1 microglia/macrophages, glial fibrillary acidic protein (GFAP) is a marker of astrocytes, and RNA binding protein fox-1 homolog 3 (neuronal nuclei antigen, NeuN) is a marker of neurons. At 1 or 5 weeks post-SCI, mice were anesthetized with 1% sodium pentobarbital (60–80 mg/kg) and sacrificed at 1 or 5 weeks post-SCI and then perfused intracardially with 20–30 mL of PBS followed by 40–60 mL of 4% paraformaldehyde. Approximately 1.5-cm-long spinal cord segments with the lesion site at the center were dissected and postfixed for 2 hours, then kept in 25% or 30% sucrose at 4°C for 2–3 days. Sagittal sections (14 μm thick) were cut using a cryostat (Cat# CM1950; Leica, Wetzlar, Germany). The slides were blocked with 3% bovine serum albumin (Cat# A8020; Solarbio) containing 0.3% Triton X-100 (MP Biomedicals, Irvine, CA, USA) and incubated at room temperature for 20 hours with the following antibodies: rabbit anti-ionized calcium-binding adapter molecule 1 (1:500, Cat# 019-19741, RRID AB_839504; FUJIFILM Wako Pure Chemical Corporation, Osaka, Japan), rabbit anti-iNOS (1:300, Cat# ab3523, RRID AB_303872; Abcam, Cambridge, UK), rabbit anti-GFAP (1:500, Cat# Z0334, RRID AB_10013382; Agilent Technologies, Santa Clara, CA, USA), rabbit anti-NeuN (1:400, Cat# ab177487, RRID AB_2532109; Abcam), goat anti-Arg-1 (1:300, Cat# sc-18354, RRID AB_2227469; Santa Cruz Biotechnology, Santa Cruz, CA, USA), goat anti-GFP (1:300, Cat#

GTX26673, RRID AB_371426; GeneTex, Irvine, CA, USA), mouse anti-NeuN (1:100, Cat# GTX30773, RRID AB_1949456; GeneTex), or mouse anti-neuron-specific class III beta-tubulin (Tuj1, 1:200, Cat# MAB1195, RRID AB_357520; R&D Systems, Minneapolis, MN, USA). After washing, the sections were incubated for 2–4 hours at room temperature with the corresponding secondary antibodies conjugated to Alexa Fluor 488 (donkey anti-mouse IgG, 10 μg/mL, Cat# 715-547-003, RRID AB_2340851; Jackson ImmunoResearch Laboratories, West Grove, PA, USA), Alexa Fluor 594 (goat anti-rabbit IgG, 10 μg/mL, Cat# 111-585-003, RRID AB_2338059; Jackson ImmunoResearch Laboratories), or DyLight 647 (donkey anti-goat IgG, 10 μg/mL, Cat# 705-605-147, RRID AB_2340437; Jackson ImmunoResearch Laboratories). Nuclei were counterstained with Hoechst 33342 (2 μg/mL, Cat# C0030; Solarbio). Images were taken under a confocal microscope (FV3000; Olympus, Tokyo, Japan).

### Locomotion evaluation

We used the Basso Mouse Scale, a nine-point scale that provides a reliable and sensitive measurement of locomotor function (with normal locomotion scored as 9 and no ankle movement scored as 0), in SCI mice to evaluate locomotion function at 0 (6 hours following injury), 7, 14, and 28 days postinjury ($n$ = 10) by two investigators blinded to the experimental design, as described (Basso et al., 2006).

### Western blot assay

Macrophages and NSCs were lysed with radioimmunoprecipitation assay buffer (0.1% sodium dodecyl sulfate, 50 mM Tris-HCl, 150 mM NaCl, 1% Triton X-100, 0.5% sodium deoxycholate, 1 mM dithiothreitol, and 5 mM ethylenediaminetetraacetic acid, pH 8.0; Beyotime Biotechnology, Shanghai, China) containing a protease inhibitor mixture of 5 mM sodium fluoride, 1 mM phenylmethylsulfonyl fluoride (MilliporeSigma), and 0.1 mg/mL aprotinin. Proteins were separated by 10% sodium dodecyl sulfate-polyacrylamide gel electrophoresis and transferred onto polyvinylidene difluoride membranes (MilliporeSigma). Before incubating with primary antibodies, membranes were blocked with 5% nonfat milk for 1 hour. The samples were incubated at 4°C overnight with rabbit anti-iNOS (1:500, Cat# ab3523, RRID AB_303872; Abcam), goat anti-Arg-1 (1:500, Cat# sc-18354, RRID AB_2227469; Santa Cruz Biotechnology), mouse anti-Tuj1 (1:500, Cat# MAB1195, RRID AB_357520; R&D Systems), rabbit anti-GFAP (1:1000, Cat# Z0334, RRID AB_10013382; Agilent Technologies), or mouse anti-β-actin (1:50 000, Cat# A5441, RRID AB_476744; MilliporeSigma). After washing three times with Tris-buffered saline + Tween-20, membranes were incubated for 1 hour at room temperature with corresponding secondary goat anti-mouse/rabbit antibodies conjugated to horseradish peroxidase (1:5000, Cat# 115-035-003, RRID AB_2313567; and Cat# 111-035-045, RRID AB_2337938; Jackson ImmunoResearch Laboratories) or rabbit anti-goat antibodies conjugated to horseradish peroxidase (Cat# 305-035-045, RRID AB_2339403; Jackson ImmunoResearch Laboratories). Bands were visualized using an enhanced chemiluminescence kit (Promega, Madison, WI, USA) and detected with the Bio-Rad ChemiDoc XRS+ (Bio-Rad Laboratories, Hercules, CA, USA). ImageJ 1.52a (Java 1.8.0_112; https://imagej.net/contribute/citing) was used to quantify optical densities.

### Real-time polymerase chain reaction

Total RNA was extracted from injured spinal tissue 7 days after NSC transplantation or from macrophages 48 hours after M1/M2 induction. After reverse transcription using a master mix (Cat# RR036A; Takara Biomedical Technology, Beijing, China), real-time polymerase chain reaction (RT-PCR) was performed. mRNA levels of target genes normalized to β-actin were evaluated by the ΔCt method, as described (Wang et al., 2011). Primers were designed by Primer-BLAST (National Center for Biotechnology Information, Bethesda, MD, USA) and synthesized by Shenggong Co., Shanghai, China. The sequences of the primers are as follows (Ye et al., 2012): β-actin, forward 5′-AGA AGG ACT CCT ATG TGG GTG A-3′, reverse 5′-CAT GAG CTG GGT CAT CTT TTC A-3′; iNOS, forward 5′-CCC TTC AAT GGT TGG TAC ATG G-3′, reverse 5′-ACA TTG ATC TCC GTG ACA GCC-3′; Arg1, forward 5′-GAA CAC GGC AGT GGC TTT AAC-3′, reverse 5′-TGC TTA GCT CTG TCT GCT TTG C-3′; Cd206, forward 5′-TCT TTG CCT TTC CCA GTC TCC-3′, reverse 5′-TGA CAC CCA GCG GAA TTT C-3′; Cd86, forward 5′-TTG TGT GTG TTC TGG AAA CGG AG-3′, reverse 5′-AAC TTA GAG GCT GTG TTG CTG GG-3′; gfap, forward 5′- CCC TGG CTC GTG TGG ATT T-3′, reverse 5′-GAC CGA TAC CAC TCC TCT GTC-3′; tuj1, forward 5′- CCC AGC GGC AAC TAT GTA GG-3′, reverse 5′-CCA GAC CGA ACA CTG TCC A-3′.

### Flow cytometry analysis

Mononuclear cells were isolated from spinal cord tissue using Percoll (Cat# 17-0891-09; MilliporeSigma) and gradient centrifugation 7 days post-SCI. The isolated microglia/macrophages were incubated in blocking solution (rat serum; Thermo Fisher Scientific) for 20 minutes at 4°C and subsequently stained with fluorescein isothiocyanate-conjugated anti-CD11b and phycoerythrin-conjugated anti-CD86 or phycoerythrin-conjugated anti-CD206 (Thermo Fisher Scientific) in darkness for 20 minutes at 4°C. Acquisitions were performed on a 6HT Guava flow cytometer (MilliporeSigma). Subsequent data were analyzed using FlowJo software (version 7.6.2; Tree Star, Ashland, OR, USA).

### Statistical analysis

No statistical methods were used to predetermine sample sizes; however, our sample sizes are similar to those reported in a previous publication (Cao et al., 2021). No mice died during our experiments. The data are presented as mean ± standard error (SE). Normality was assessed by the Shapiro-Wilk test. Homogeneity of variance was evaluated by Levene's test. For data that met normality and homogeneity of variance, one-way analysis of variance or Student's $t$-test were performed. For data that did not meet normality and homogeneity of variance, we used the Kruskal-Wallis $H$ test, the Mann-Whitney $U$ test, or the Wilcoxon signed-rank test. Data were analyzed using SPSS for Windows, version 16.0 (SPSS, Chicago, IL, USA). $P$-values less than 0.05 were considered statistically significant. Statistical analysis was conducted by researchers blinded to the experimental design.

## Results

### Glial differentiation of transplanted NSCs in M1 microglia/macrophage-dominated spinal cord

Neurons died quickly in the lesion center following SCI, as previously reported (Tran et al., 2018). There were almost no NeuN-positive cells in the epicenter at 1 week postinjury (wpi) (**Additional Figure 1A**). To test if NSC transplantation could replenish the lost neurons, GFP-labeled NSCs were transplanted into the lesion center at 24 hours postinjury, and cell fate was examined at 1 and 5 wpi. At both time points, most of the GFP-positive cells expressed GFAP (**Figure 1A** and **Additional Figure 1B**). NeuN/GFP-positive neurons were very rarely detected, indicating that NSCs transplanted into injured spinal cord primarily gave rise to astrocytes (**Figure 1A**). Notably, the number of GFP-positive NSCs was smaller at 5 wpi than at 1 wpi (**Figure 1A** and **Additional Figure 1C**).

To reveal the underlying mechanism, we focused on the role of inflammation, especially in regard to the fate of microglia/macrophages in the lesion site, because it has been shown that the polarization of microglia/macrophages significantly affects the survival and differentiation of NSCs in the hippocampus and subventricular zone (Choi et al., 2017; Mecha et al., 2020). At 1 wpi, there were numerous iNOS-positive cells (M1 microglia/macrophages) and a smaller number of Arg-1-positive cells (M2 microglia/macrophages) in the lesion area (**Figure 1B**), indicating M1 microglia/macrophage-dominated inflammation. At 5 wpi, the population of M1 microglia/macrophages persisted, whereas the total number of M1 and M2 microglia/macrophages reduced compared with those at 1 wpi (**Figure 1B**). These data demonstrate an astrocytic fate of transplanted NSCs in the M1 microglia/macrophage-dominated injured spinal cord.

### Promotion of neuronal differentiation of NSCs by M2 microglia/macrophages

As the polarization of microglia modulates the differentiation of NSCs in the hippocampus and subventricular zone (Choi et al., 2017; Mecha et al., 2020), we assessed the effects of M0, M1, and M2 macrophages on the differentiation of spinal cord NSCs *in vitro*. Immunocytochemistry showed that there were significantly fewer Tuj1-positive cells in NSCs treated with M1-CM ($P$ < 0.01) than in NSCs treated with M0-CM (**Figure 2A–C**). In contrast, significantly fewer GFAP-positive cells ($P$ < 0.01) and significantly more Tuj1-positive cells were found in NSCs treated with M2-CM ($P$ < 0.001) than in NSCs treated with M0-CM (**Figure 2A–C**). RT-PCR showed similar changes in Gfap and Tuj1 gene expression (**Figure 2D** and **E**). These data indicate that M1 microglia/macrophages favor glial differentiation, whereas M2 microglia/macrophages support neuronal differentiation.
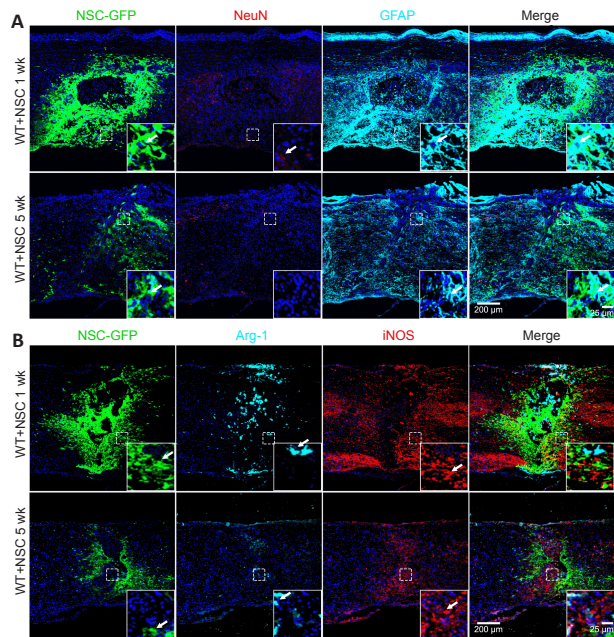
**Figure 1 | Astrocytic differentiation of NSCs and M1-dominated microglia/macrophages in injured spinal cord of mice.**
(A) Triple immunostaining of GFP/NeuN/GFAP at 1 and 5 weeks after NSC transplantation. GFP-labeled NSCs expressed GFAP. Almost no GFP/NeuN-positive cells were observed at both time points. GFP: Green; NeuN: red, stained with Alexa Fluor 594; GFAP: light blue, stained with Alexa Fluor 647, converted into virtual color. (B) Triple immunostaining of GFP/Arg-1/iNOS at 1 and 5 weeks post-injury. There were more iNOS-positive cells than Arg-1-positive cells in the lesion area at both time points. GFP: Green; Arg-1: light blue, stained with Alexa Fluor 647, converted into virtual color; iNOS: red, stained with Alexa Fluor 594. Images in dashed frames were magnified. Arrows show typical immunopositive cells. Scale bars: 200 µm (main image) and 25 µm (in insert). Arg-1: Arginase-1; GFAP: glial fibrillary acidic protein; GFP: green fluorescent protein; iNOS: inducible nitric oxide synthase; NSC: neural stem cell; WT: wild type.
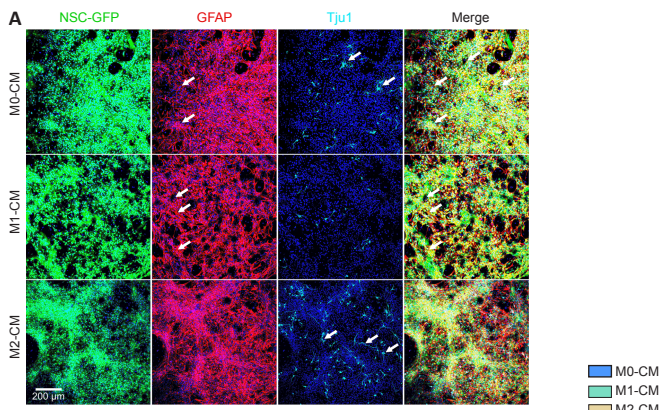


**Figure 2 | Effects of macrophage polarization on the differentiation of NSCs.**
(A) Triple immunostaining of GFP/GFAP/Tuj1 in NSCs treated with M0-CM, M1-CM, and M2-CM. There were more Tuj1-positive cells in NSCs treated with M2-CM and more GFAP-positive cells in NSCs treated with M1-CM. GFP: Green; GFAP: red, stained with Alexa Fluor 594; Tuj1: light blue, stained with Alexa Fluor 647, converted into virtual color. Arrows show typical immunopositive cells. Scale bars: 200 µm. (B, C) Percentage of GFAP- or Tuj1-positive cells. (D, E) Real-time polymerase chain reaction of Gfap (D) and Tuj1 (E) in NSCs treated with M0-CM, M1-CM, and M2-CM. Relative mRNA expression was normalized by the internal control, β-actin. Data are expressed as mean ± SE (*n* = 3 batches of cells per group). #*P* < 0.05, ##*P* < 0.01, ###*P* < 0.001 (one-way analysis of variance followed by Tukey's *post hoc* test). CM: Conditioned medium; GFAP: glial fibrillary acidic protein; GFP: green fluorescent protein; M0: untreated macrophage; M1: M1 phenotype macrophage; M2: M2 phenotype macrophage; NSC: neural stem cell; Tuj1: β-tubulin III.

## Long-term M2 microglia/macrophages and neuronal differentiation of NSCs in aldose reductase-deficient spinal cord

A previous study reported that an AR mutation influenced the polarization of macrophages in the early phase of SCI (Zhang et al., 2016). We examined changes in the long-term fate of microglia/macrophages in AR-deficient mice after SCI. Using triple immunostaining, we detected large numbers of iNOS-positive cells in WT mice at 5 wpi, but we detected only a small number of iNOS-positive cells in the injured spinal cord of AR-deficient mice at 5 wpi (**Figure 3A–D**). In contrast, more Arg-1-positive cells were detected in the lesion area of AR-deficient spinal cord at 5 wpi than in the WT spinal cord (**Figure 3A–D**). Flow cytometry analysis of CD86 and CD206, markers of M1 and M2 macrophages (Xu et al., 2019), respectively, confirmed the M2-dominated inflammation in AR-deficient spinal cord (**Additional Figure 2**). These data indicate that AR deficiency resulted in a long-term M2 polarization of microglia/macrophages in the injured spinal cord.
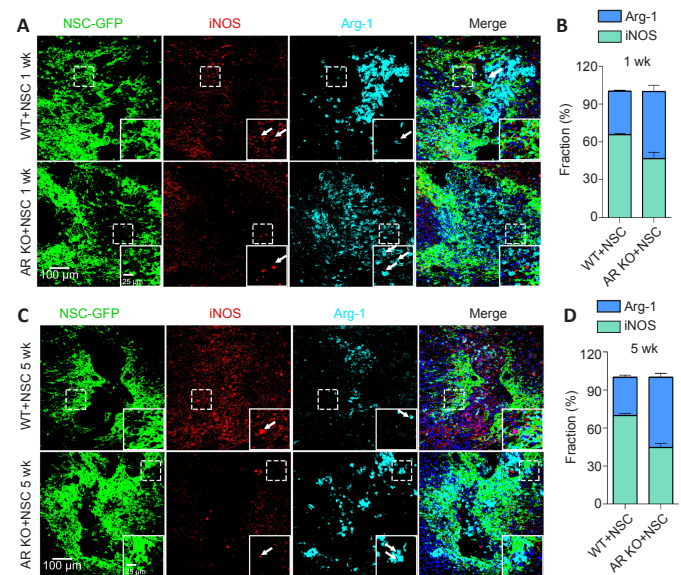


**Figure 3 | Long-term M2 polarization of microglia/macrophages in spinal cord of AR-deficient mice.**
(A, B) Triple immunostaining and quantification of GFP/iNOS/Arg-1 at 1 week after NSC transplantation in WT and AR-deficient mice. (C, D) Triple immunostaining and quantification of GFP/iNOS/Arg-1 at 5 weeks after NSC transplantation in WT and AR-deficient mice. There was a higher percentage of Arg-1-positive cells in AR-deficient mice than in WT mice at both time points. Images in dashed frames were magnified. GFP: Green; iNOS: red, stained with Alexa Fluor 594; Arg-1: light blue, stained with Alexa Fluor 647, converted into virtual color. Arrows show typical immunopositive cells. Scale bars: 100 µm (main image) and 25 µm (in insert). Data are expressed as mean ± SE (*n* = 4 mice per group) and were analyzed by Student's *t*-test. AR: Aldose reductase; AR KO: AR-deficient mice; Arg-1: arginase-1; GFP: green fluorescent protein; iNOS: inducible nitric oxide synthase; NSC: neural stem cell; WT: wild type.

We then investigated the fate of transplanted GFP-NSCs in AR-deficient spinal cord. GFP-NSCs transplanted in AR-deficient mice generated large numbers of neurons at 1 wpi (*P* < 0.001) compared with cells transplanted in WT mice, as showed by GFP/NeuN double immunostaining (**Figure 4A–C**). At 5 wpi, the number of GFP/NeuN-positive cells remained high, indicating a high efficiency of neuronal differentiation of exogenous NSCs in AR-deficient spinal cord and a better survival of new neurons (**Figure 4B** and **C**). At both time points, the numbers of GFP/GFAP-positive cells in AR-deficient mice were smaller than in WT mice (*P* < 0.001 at 1 wpi, and *P* < 0.01 at 5 wpi; **Figure 4D**). Consistent with these results, AR-deficient mice with NSC transplantation had significantly higher Basso Mouse Scale scores than WT mice with NSC transplantation from 1 wpi (*P* < 0.01 at 1 and 4 wpi, *P* < 0.05 at 2 and 3 wpi; **Figure 4E**). These data demonstrate that AR mutation in host mice could result in long-term M2 polarization of microglia/macrophages and efficient neuronal differentiation of NSC transplants.
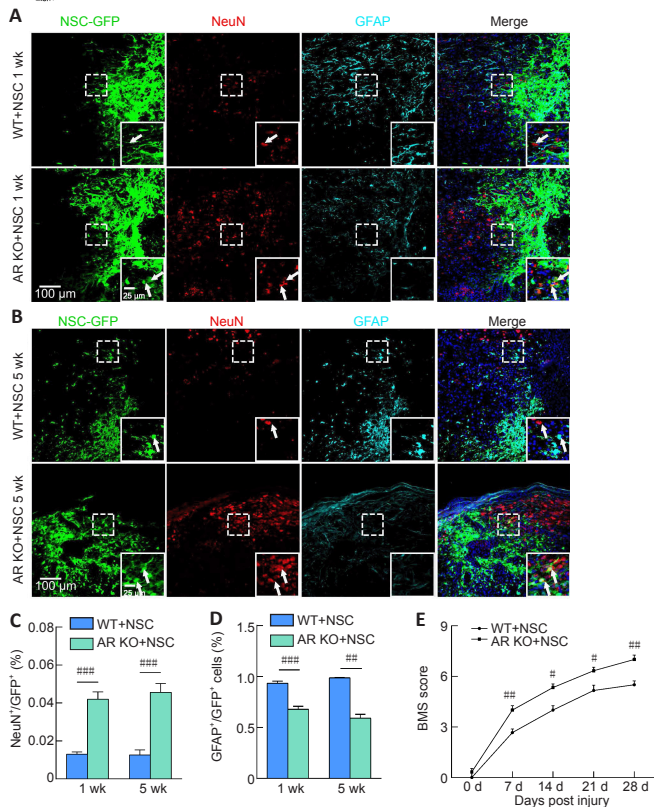
**Figure 4 | Long-term neuronal differentiation of NSCs transplanted in AR-deficient spinal cord.**

(A) Triple immunostaining of GFP/NeuN/GFAP in WT and AR-deficient mice at 1 week after NSC transplantation. Robust neuronal differentiation of NSCs was found in the injured spinal cord of AR-deficient mice. (B) Triple immunostaining of GFP/NeuN/GFAP in WT and AR-deficient mice at 5 weeks after transplantation. Large numbers of GFP/NeuN-positive cells were seen in the lesion area of AR-deficient mice. GFP: Green; NeuN: red, stained with Alexa Fluor 594; GFAP: light blue, stained with Alexa Fluor 647, converted into virtual color. Arrows show typical immunopositive cells. Scale bars: 100 μm (main image) and 25 μm (in insert). (C, D) Quantification of GFP/NeuN-positive cells and GFP/GFAP-positive cells at 1 and 5 weeks after transplantation. The percentage of GFP/NeuN-positive cells was increased and GFP/GFAP-positive cells was decreased in AR-deficient mice compared with WT mice. (E) Basso Mouse Scale scoring of WT and AR-deficient mice with NSC transplantation. Data are expressed as mean ± SE ($n$ = 6 mice per group). #$P$ < 0.05, ##$P$ < 0.01, ###$P$ < 0.001 (one-way analysis of variance followed by Tukey's *post hoc* test). AR: Aldose reductase; AR KO: AR-deficient mice; Arg-1: arginase-1; GFAP: glial fibrillary acidic protein; GFP: green fluorescent protein; NSC: neural stem cell; WT: wild type.

## M2 polarization of microglia/macrophages and neuronal differentiation of NSCs in AR-inhibited spinal cord

Considering the future application of NSC transplantation in the clinic, we next investigated the effects of pharmacological inhibition of host AR activity on microglia/macrophage polarization and neuronal differentiation. Application of sorbinil (1 nM) to the culture medium of primary macrophages significantly increased the gene expression levels of Arg1 ($P$ < 0.05) and Cd206 ($P$ < 0.01) in M2-primed macrophages (**Figure 5A** and **B**) and suppressed the levels of Cd86 ($P$ < 0.05) and iNOS ($P$ < 0.001) in M1-primed macrophages (**Figure 5C** and **D**). Sorbinil treatment significantly increased the protein expression of Arg-1 in both naïve and M1/M2-primed macrophages (**Figure 5E–G**). These data indicate that sorbinil treatment could effectively bias the differentiation of macrophages toward the M2 phenotype *in vitro*.

We next evaluated whether macrophages with inhibited AR activity affected the fate of NSCs by stimulating NSCs with CM collected from naïve macrophages or from macrophages pretreated with sorbinil. Western blot revealed that M2-CM from sorbinil-pretreated macrophages significantly increased the expression of Tuj1 in NSCs ($P$ < 0.01). CM from sorbinil-pretreated macrophages significantly reduced the expression of GFAP in NSCs ($P$ < 0.05 in M1-CM, $P$ < 0.01 in M2-CM; **Figure 6A–C**).

For our *in vivo* study, three doses of sorbinil were administered 1 day before, immediately after, and 1 day after NSC transplantation
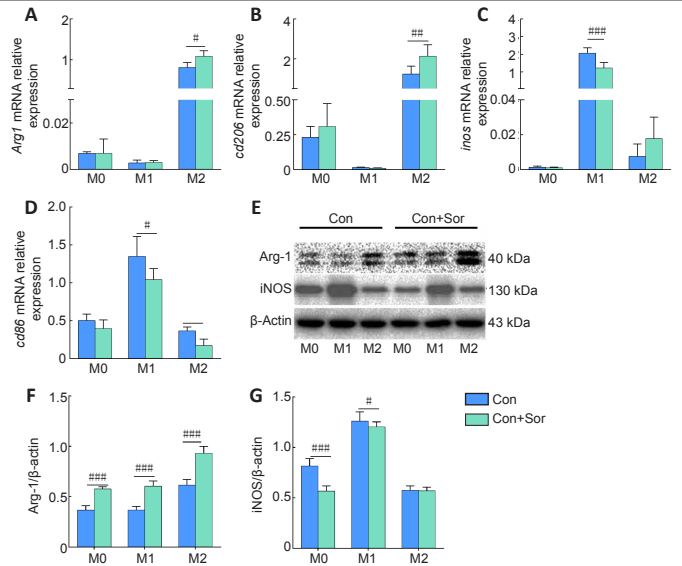


**Figure 5 | Effects of AR inhibition on the polarization of macrophages *in vitro*.**

(A–D) Real-time polymerase chain reaction of Arg1, Cd206, iNOS, and Cd86 levels in macrophages treated with or without sorbinil. Relative mRNA expression was normalized to the internal control, β-actin. (E–G) Western blots of Arg-1 and iNOS in macrophages treated with or without sorbinil. Data are expressed as mean ± SE ($n$ = 3 batches of cells per group). #$P$ < 0.05, ##$P$ < 0.01, ###$P$ < 0.001 (one-way analysis of variance followed by Tukey's *post hoc* test). AR: Aldose reductase; Arg-1/Arg1: arginase-1; Con: control; iNOS: inducible nitric oxide synthase; M0: untreated macrophage; M1: M1 phenotype macrophage; M2: M2 phenotype macrophage; Sor: sorbinil.
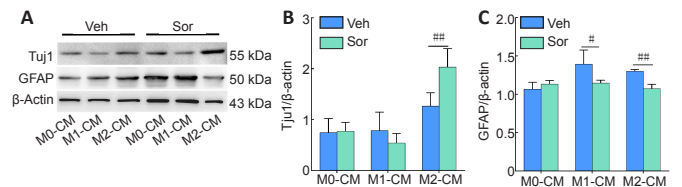


**Figure 6 | Differentiation of NSCs by stimulation of sorbinil-pretreated macrophages.**

(A) Western blots of Tuj1 and GFAP in NSCs treated with conditioned medium collected from M0-, M1-, or M2-primed macrophages that were pretreated with or without sorbinil. (B, C) Quantification of Tuj1 and GFAP expression. Data are expressed as mean ± SE ($n$ = 3 batches of cells per group). #$P$ < 0.05, ##$P$ < 0.01 (one-way analysis of variance followed by Tukey's *post hoc* test). CM: Conditioned medium; GFAP: glial fibrillary acidic protein; M0: untreated macrophage; M1: M1 phenotype macrophage; M2: M2 phenotype macrophage; Sor: sorbinil; Tuj1: neuron-specific class III beta-tubulin; Veh: vehicle.

(**Figure 7A**). At 1 wpi, sorbinil-treated spinal cord had remarkably reduced numbers of iNOS-positive cells and increased numbers of Arg-1-positive cells (**Figure 7B** and **C**), indicating that sorbinil treatment was effective in inducing M2 macrophages *in vivo*. GFP/NeuN double staining showed that there were significantly more NeuN/GFP-positive cells in spinal cords treated with NSC-sorbinil than for NSC-PBS (**Figure 7D** and **E**). Behavior analysis showed that mice treated with NSC-sorbinil displayed significantly higher Basso Mouse Scale scores from 1 wpi compared with mice treated with NSC transplantation or PBS (**Figure 7F**). These data indicate that AR inhibition could be adopted to induce M2 microglia/macrophages and neuronal differentiation of NSC transplants after SCI.

## Discussion

Here, we first demonstrated an astrocytic differentiation of transplanted NSCs and an M1-dominated microenvironment in injured spinal cord. Then, we reported a long-term M2 polarization of microglia/macrophages in AR-deficient mice after SCI. Based on this observation, we evaluated the neuronal differentiation of NSCs in AR-deficient and AR-suppressed mice. Our data show that inhibition of host AR activity remarkably increased neuronal differentiation of NSCs in injured spinal cord and significantly improved functional recovery.
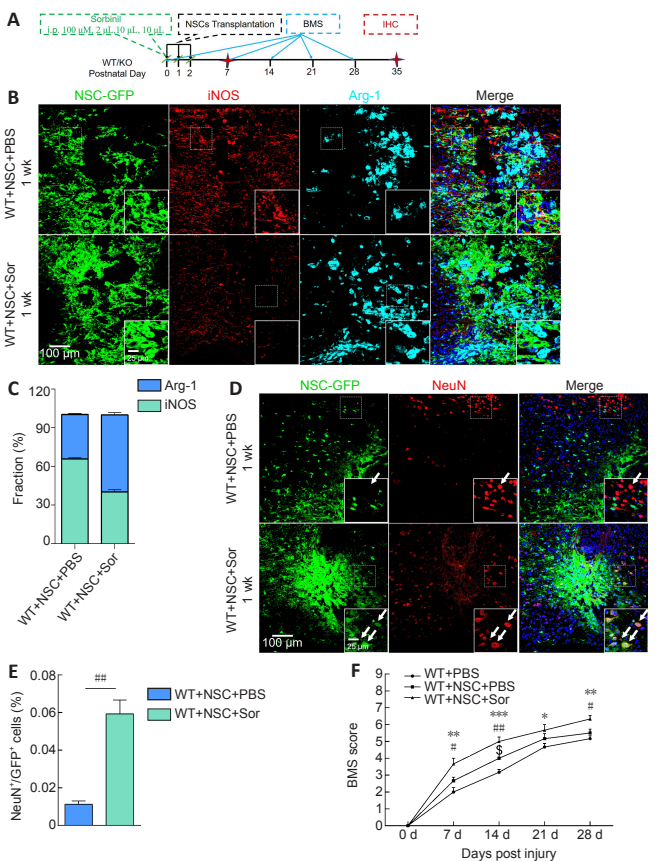
**Figure 7 | M2-polarization of microglia/macrophages and neuronal differentiation of transplanted NSCs in AR-inhibited spinal cord.**

(A) Scheme of experimental design. (B) Triple immunostaining of GFP/iNOS/Arg-1 in mice treated with vehicle or sorbinil at 1 week after transplantation. GFP: green; iNOS: red, stained with Alexa Fluor 594; Arg-1: light blue, stained with Alexa Fluor 647, converted into virtual color. (C) Quantification of iNOS and Arg-1. (D) Double immunostaining of GFP/NeuN in mice treated with vehicle or sorbinil at 1 week after transplantation. GFP: Green; NeuN: red, stained with Alexa Fluor 594. Arrows show typical immunopositive cells. Scale bars: 100 μm (main image) and 25 μm (in insert). (E) Quantification of GFP/NeuN-positive cells. (F) Basso Mouse Scale scoring. Data are expressed as mean ± SE ($n$ = 8 mice in WT-NSC-PBS group, 10 mice in WT-NSC-sorbinil group and in WT-PBS group). #$P < 0.05$, ##$P < 0.01$, $vs$. NSC-PBS group; *$P < 0.05$, **$P < 0.01$, ***$P < 0.001$, $vs$. PBS group (one-way analysis of variance followed by Bonferroni $post hoc$ test). AR: Aldose reductase; Arg-1: arginase-1; BMS: Basso Mouse Scale; GFP: green fluorescent protein; IHC: immunohistochemistry; iNOS: inducible nitric oxide synthase; KO: AR-deficient mice; NSC: neural stem cell; PBS: phosphate-buffered saline; Sor: sorbinil; WT: wild type.

The highlight of this study is the robust neuronal differentiation of transplanted NSCs in injured spinal cord. Injured spinal cord is hostile to neurogenesis. Ke et al. (2006) reported that endogenous progenitor cells in the spinal cord actively responded to injury but only gave rise to astrocytes and oligodendrocytes. The lack of neuron-inductive factors and the upregulation of gliogenic factors (such as bone morphogenetic protein) by reactive astrocytes were thought to account for the gliogenic microenvironment of injured spinal cord (Noble et al., 2011; Hart et al., 2020). Many studies have been conducted to supply neural inductive factors (such as epithelial growth factor and Wnt) or to antagonize gliogenic factors (such as inhibition of Notch signaling) (Khazaei et al., 2020; Younsi et al., 2020). In the present study, we achieved robust neuronal differentiation from transplanted NSCs by inhibiting host AR activity or by depleting host AR. As AR was knocked out or inhibited globally, we did not exclude the effects of the change of bone morphogenetic protein/Notch signaling in AR-deficient mice. The persistence of large numbers of NeuN/GFP-positive cells at 5 wpi indicated the survival and maturation of new neurons. The enhanced recovery of locomotion at 1 wpi also implied better survival of residual neurons, which was possible as M2 microglia/macrophages have been shown to be neuroprotective (Franco and Fernández-Suárez, 2015; Chen

and Trapp, 2016). A limitation of our study is the use of mice with global AR deficiency. The roles of AR in other cell types could not be excluded. Nevertheless, our data suggest that modulation of AR activity might provide a favorable microenvironment for NSC transplantation. Whether these neurons bear the properties of spinal motor neurons or integrate into the spinal circuit remains to be investigated.

As a key enzyme that regulates glucose metabolism, AR is reportedly upregulated in diabetic retinopathy; inhibition of AR activity blocks tumor necrosis factor secretion and microglia activation (Chang et al., 2019). Recently, studies have revealed that AR participates in multiple inflammatory diseases by regulating the production of reactive oxygen species and cytokines/chemokines (Chatzopoulou et al., 2013). As AR is rapidly upregulated in microglia/macrophages after SCI (Zhang et al., 2016), and glucose metabolism is important for polarization of microglia/macrophages (Van den Bossche et al., 2017), we evaluated the long-term effects of AR deficiency or inhibition on the fate of microglia/macrophages. In the hippocampus and cerebral cortex, M2 microglia/macrophages reportedly stimulate neurogenesis from NSCs in the dentate gyrus and subventricular zone by releasing brain-derived neurotrophic factor or activating Wnt signaling (Xiong et al., 2016; Yang et al., 2019; Gampierakis et al., 2021). Because the spinal cord lacks endogenous NSCs, our data of long-term persistence of M2 microglia/macrophages in AR-deficient spinal cord inspired the idea of combining an AR inhibitor with NSC transplantation. Importantly, three doses of sorbinil dramatically prolonged the M2 phenotype for greater than one month and simultaneously suppressed the M1 fate of microglia/macrophages, which greatly facilitated the neuronal differentiation and survival of transplanted NSCs. Whether the newly differentiated neurons can form synaptic connections with endogenous circuits needs to be further investigated.

Inhibition of host AR activity in combination with NSC transplantation may also affect other inflammatory cells and help to reduce immune rejection. In addition, some natural compounds and plant extracts inhibit AR activity. Therefore, it would be worthwhile to test a combination of other AR inhibitors used in the clinic with NSC transplantation for the treatment of SCI.

**Conflicts of interest:** *The authors claim no conflicts of interests.*
**Availability of data and materials:** *All data generated or analyzed during this study are included in this published article and its supplementary information files.*
**Open peer reviewer:** *Hedong Li, Augusta University, USA.*
**Additional files:**
*Additional Figure 1:* *Neuronal survival in the lesion area and differentiation of NSCs in injured spinal cord.*
*Additional Figure 2:* *Flow cytometry analysis of CD206 (M2 marker; left) and CD86 (M1 marker; right) in WT and AR-deficient spinal cord at 1 week post-spinal cord injury.*
*Additional file 1:* *Open peer review report 1.*

# References

Abecassis ZA, Berceau BL, Win PH, García D, Xenias HS, Cui Q, Pamukcu A, Cherian S, Hernández VM, Chon U, Lim BK, Kim Y, Justice NJ, Awatramani R, Hooks BM, Gerfen CR, Boca SM, Chan CS (2020) Npas1(+)-Nkx2.1(+) Neurons are an integral part of the cortico-pallido-cortical Loop. J Neurosci 40:743-768.

Albers JW, Pop-Busui R (2014) Diabetic neuropathy: mechanisms, emerging treatments, and subtypes. Curr Neurol Neurosci Rep 14:473.

Alexiou P, Pegklidou K, Chatzopoulou M, Nicolaou I, Demopoulos VJ (2009) Aldose reductase enzyme and its implication to major health problems of the 21(st) century. Curr Med Chem 16:734-752.

Assinck P, Duncan GJ, Hilton BJ, Plemel JR, Tetzlaff W (2017) Cell transplantation therapy for spinal cord injury. Nat Neurosci 20:637-647.

Basso DM, Fisher LC, Anderson AJ, Jakeman LB, McTigue DM, Popovich PG (2006) Basso Mouse Scale for locomotion detects differences in recovery after spinal cord injury in five common mouse strains. J Neurotrauma 23:635-659.

Cao X, Wang Y, Gao L (2021) CHRFAM7A overexpression attenuates cerebral ischemia-reperfusion injury via inhibiting microglia pyroptosis mediated by the NLRP3/Caspase-1 pathway. Inflammation 44:1023-1034.

Carter LJ, Garner LV, Smoot JW, Li Y, Zhou Q, Saveson CJ, Sasso JM, Gregg AC, Soares DJ, Beskid TR, Jervey SR, Liu C (2020) Assay techniques and test development for COVID-19 diagnosis. ACS Cent Sci 6:591-605.

Chang KC, Shieh B, Petrash JM (2019) Role of aldose reductase in diabetes-induced retinal microglia activation. Chem Biol Interact 302:46-52.

Chatzopoulou M, Pegklidou K, Papastavrou N, Demopoulos VJ (2013) Development of aldose reductase inhibitors for the treatment of inflammatory disorders. Expert Opin Drug Discov 8:1365-1380.

Chen Z, Trapp BD (2016) Microglia and neuroprotection. J Neurochem 136 Suppl 1:10-17.

Choi JY, Kim JY, Kim JY, Park J, Lee WT, Lee JE (2017) M2 Phenotype microglia-derived cytokine stimulates proliferation and neuronal differentiation of endogenous stem cells in ischemic brain. Exp Neurobiol 26:33-41.

Fan B, Wei Z, Yao X, Shi G, Cheng X, Zhou X, Zhou H, Ning G, Kong X, Feng S (2018) Microenvironment imbalance of spinal cord injury. Cell Transplant 27:853-866.

Fan H, Liu X, Tang HB, Xiao P, Wang YZ, Ju G (2013) Protective effects of Batroxobin on spinal cord injury in rats. Neurosci Bull 29:501-508.

Franco R, Fernández-Suárez D (2015) Alternatively activated microglia and macrophages in the central nervous system. Prog Neurobiol 131:65-86.

Gampierakis IA, Koutmani Y, Semitekolou M, Morianos I, Polissidis A, Katsouda A, Charalampopoulos I, Xanthou G, Gravanis A, Karalis KP (2021) Hippocampal neural stem cells and microglia response to experimental inflammatory bowel disease (IBD). Mol Psychiatry 26:1248-1263.

Hart CG, Dyck SM, Kataria H, Alizadeh A, Nagakannan P, Thliveris JA, Eftekharpour E, Karimi-Abdolrezaee S (2020) Acute upregulation of bone morphogenetic protein-4 regulates endogenous cell response and promotes cell death in spinal cord injury. Exp Neurol 325:113163.

Ho HT, Chung SK, Law JW, Ko BC, Tam SC, Brooks HL, Knepper MA, Chung SS (2000) Aldose reductase-deficient mice develop nephrogenic diabetes insipidus. Mol Cell Biol 20:5840-5846.

Ke Y, Chi L, Xu R, Luo C, Gozal D, Liu R (2006) Early response of endogenous adult neural progenitor cells to acute spinal cord injury in mice. Stem Cells 24:1011-1019.

Khazaei M, Ahuja CS, Nakashima H, Nagoshi N, Li L, Wang J, Chio J, Badner A, Seligman D, Ichise A, Shibata S, Fehlings MG (2020) GDNF rescues the fate of neural progenitor grafts by attenuating Notch signals in the injured spinal cord in rodents. Sci Transl Med 12:eaau3538.

Liu S, Xie YY, Wang LD, Tai CX, Chen D, Mu D, Cui YY, Wang B (2021) A multi-channel collagen scaffold loaded with neural stem cells for the repair of spinal cord injury. Neural Regen Res 16:2284-2292.

Lu P, Kadoya K, Tuszynski MH (2014) Axonal growth and connectivity from neural stem cell grafts in models of spinal cord injury. Curr Opin Neurobiol 27:103-109.

Mecha M, Yanguas-Casás N, Feliú A, Mestre L, Carrillo-Salinas FJ, Riecken K, Gomez-Nicola D, Guaza C (2020) Involvement of Wnt7a in the role of M2c microglia in neural stem cell oligodendrogenesis. J Neuroinflammation 17:88.

Noble M, Davies JE, Mayer-Pröschel M, Pröschel C, Davies SJ (2011) Precursor cell biology and the development of astrocyte transplantation therapies: lessons from spinal cord injury. Neurotherapeutics 8:677-693.

Orr MB, Gensel JC (2018) Spinal cord injury scarring and inflammation: therapies targeting glial and inflammatory responses. Neurotherapeutics 15:541-553.

Quattrini L, La Motta C (2019) Aldose reductase inhibitors: 2013-present. Expert Opin Ther Pat 29:199-213.

Sabelström H, Stenudd M, Réu P, Dias DO, Elfineh M, Zdunek S, Damberg P, Göritz C, Frisén J (2013) Resident neural stem cells restrict tissue damage and neuronal loss after spinal cord injury in mice. Science 342:637-640.

Stunault MI, Bories G, Guinamard RR, Ivanov S (2018) Metabolism plays a key role during macrophage activation. Mediators Inflamm 2018:2426138.

Tran AP, Warren PM, Silver J (2018) The biology of regeneration failure and success after spinal cord injury. Physiol Rev 98:881-917.

Van den Bossche J, O'Neill LA, Menon D (2017) Macrophage immunometabolism: where are we (going)? Trends Immunol 38:395-406.

Venkatesh K, Ghosh SK, Mullick M, Manivasagam G, Sen D (2019) Spinal cord injury: pathophysiology, treatment strategies, associated challenges, and future implications. Cell Tissue Res 377:125-151.

Wang GY, Cheng ZJ, Yuan PW, Li HP, He XJ (2021) Olfactory ensheathing cell transplantation alters the expression of chondroitin sulfate proteoglycans and promotes axonal regeneration after spinal cord injury. Neural Regen Res 16:1638-1644.

Wang YZ, Yamagami T, Gan Q, Wang Y, Zhao T, Hamad S, Lott P, Schnittke N, Schwob JE, Zhou CJ (2011) Canonical Wnt signaling promotes the proliferation and neurogenesis of peripheral olfactory stem cells during postnatal development and adult regeneration. J Cell Sci 124:1553-1563.

World Health Organization (2013) Spinal cord injury. https://www.who.int/news-room/fact-sheets/detail/spinal-cord-injury. Accessed August 23, 2021.

Xiong XY, Liu L, Yang QW (2016) Functions and mechanisms of microglia/macrophages in neuroinflammation and neurogenesis after stroke. Prog Neurobiol 142:23-44.

Xu Y, Jiang Y, Wang L, Huang J, Wen J, Lv H, Wu X, Wan C, Yu C, Zhang W, Zhao J, Zhou Y, Chen Y (2019) Thymosin alpha-1 inhibits complete Freund's adjuvant-induced pain and production of microglia-mediated pro-inflammatory cytokines in spinal cord. Neurosci Bull 35:637-648.

Yang Y, Ye Y, Kong C, Su X, Zhang X, Bai W, He X (2019) MiR-124 enriched exosomes promoted the M2 polarization of microglia and enhanced hippocampus neurogenesis after traumatic brain injury by inhibiting TLR4 pathway. Neurochem Res 44:811-828.

Ye J, Coulouris G, Zaretskaya I, Cutcutache I, Rozen S, Madden TL (2012) Primer-BLAST: a tool to design target-specific primers for polymerase chain reaction. BMC Bioinformatics 13:134.

Younsi A, Zheng G, Scherer M, Riemann L, Zhang H, Tail M, Hatami M, Skutella T, Unterberg A, Zweckberger K (2020) Three growth factors induce proliferation and differentiation of neural precursor cells in vitro and support cell-transplantation after spinal cord injury in vivo. Stem Cells Int 2020:5674921.

Zhang Q, Bian G, Chen P, Liu L, Yu C, Liu F, Xue Q, Chung SK, Song B, Ju G, Wang J (2016) Aldose reductase regulates microglia/macrophages polarization through the cAMP response element-binding protein after spinal cord injury in mice. Mol Neurobiol 53:662-676.